# Experimental Infection with *Schistosoma mansoni* in CCR5-Deficient Mice Is Associated with Increased Disease Severity, as CCR5 Plays a Role in Controlling Granulomatous Inflammation[∇]

Adriano L. S. Souza,[1] Patrícia R. S. Souza,[1] Cíntia A. Pereira,[2] Adriana Fernandes,[2]
Rodrigo Guabiraba,[1] Remo C. Russo,[1] Leda Q. Vieira,[1] Ary Corrêa, Jr.,[3]
Mauro M. Teixeira,[1] and Deborah Negrão-Corrêa[2]*

*Departamento de Bioquímica e Imunologia, Instituto de Ciências Biológicas, Universidade Federal de Minas Gerais, Belo Horizonte, MG, Brazil[1]; Departamento de Parasitologia, Instituto de Ciências Biológicas, Universidade Federal de Minas Gerais, Belo Horizonte, MG, Brazil[2]; and Departamento de Microbiologia, Instituto de Ciências Biológicas, Universidade Federal de Minas Gerais, Belo Horizonte, MG, Brazil[3]*

The plasma level of the chemokine CCL3 is elevated in patients with chronic severe schistosomiasis mansoni. We have previously shown that CCL3$^{-/-}$ mice with experimental infection showed diminished pathology and worm burden compared to those of wild-type (WT) mice. To elucidate further the role of CC chemokines during schistosomiasis mansoni infection, we evaluated the course of infection in C57BL/6J mice deficient in CCR5, one of the receptors for CCL3. The CCR5 deficiency proved to be remarkably deleterious to the host, since mortality rates reached 70% at 14 weeks postinfection in CCR5$^{-/-}$ mice and 19% in WT mice. The increased lethality was not associated with an increased parasite burden, since similar numbers of eggs and adult worms were found in mice from both groups. Liver granulomas of chronically infected CCR5$^{-/-}$ mice were larger and showed greater numbers of cells and collagen deposition than liver granulomas from WT mice. This was associated with higher levels of production of intereleukin-5 (IL-5), IL-13, CCL3, and CCL5 in infected CCR5$^{-/-}$ mice than in infected WT mice. Moreover, at 8 weeks after infection, just before changes in pathology and mortality, the numbers of FoxP3-positive cells were lower in liver granulomas of CCR5$^{-/-}$ mice than in WT mice. In conclusion, the CCR5 deletion is deleterious to mice infected with *Schistosoma mansoni*, and this is associated with enhanced fibrosis and granulomatous inflammation.

CCR5 is expressed on various cell types, including thymocytes (11), B cells (18), T lymphocytes (15), macrophages (13), and dendritic cells (44), and appears to play a relevant role in the migration of blood mononuclear cells (39). Ligands that exhibit high affinity for CCR5 are CCL3, CCL4, CCL5, and CCL8. In mice, CCR5 is one of the two main chemokine receptors, besides CCR1, onto which the CC chemokine CCL3 exhibits agonistic activity (34). The latter chemokine has been suggested by two previous studies of our group to play an important role in the pathogenesis of schistosomiasis. The main findings of these studies which led to this suggestion were (i) a correlation between high plasma levels of CCL3 and the occurrence of severe disease in humans (16, 42) and (ii) the development of milder infection and pathology in CCL3$^{-/-}$ mice than in wild-type (WT) controls (42, 43). Moreover, treatment with Met-RANTES, a CCR1 and CCR5 antagonist, inhibited cellular reactivity in a model of *in vitro* granuloma reactions when cells were obtained from hepatosplenic patients, while it tended to exacerbate the granuloma index in cultures derived from intestinal patients (16). To the best of our knowledge, there are no reports of the course of *Schistosoma mansoni* infection in mice that are deficient in CCR5.

CCR5 plays essential roles in the inflammatory response induced by infectious diseases. It was demonstrated previously that a mutated CCR5 allele (CCR5Δ32 homozygous) was associated with relative protection against HIV-1 transmission and pathogenesis (21). Experiments using CCR5-deficient mice showed that this chemokine receptor plays an important role in controlling local inflammation and pathogen persistence in experimental infection with *Toxoplasma gondii* (26), *Trypanosoma cruzi* (29), *Histoplasma capsulatum* (27), and *Leishmania major* (46) and in paracoccidioidomycosis (33). The two latter studies indicated that CCR5 favors the recruitment of cells with regulatory properties to the site of infection, leading to a modulation of the immune response. Given the lack of reports on the course of *S. mansoni* infection in mice that are deficient in CCR5, the evidence that CCL3, one of CCR5 ligands, is relevant in *S. mansoni* infection, and evidence from both human and animal models that CCR5 may have a role in the pathogenesis of various infectious diseases, we have infected CCR5-deficient mice to investigate further the role of CC chemokines in the context of schistosomiasis.

## MATERIALS AND METHODS

**Animals and infection.** The animals used for the experimental infections were male and female C57BL/6J mice from the animal facility of the Universidade Federal de Minas Gerais (UFMG), and CCR5-deficient mice (47) in the C57BL/6J background, purchased from the Jackson Laboratories (Bar Harbor,

* Corresponding author. Mailing address: Departamento de Parasitologia, Instituto de Ciências Biológicas, Universidade Federal de Minas Gerais, Av. Antônio Carlos 6627, CEP 30882-650-Pampulha, Belo Horizonte, MG, Brazil. Phone and fax: 55 31 3409 2855. E-mail: denegrao@icb.ufmg.br.
∇ Published ahead of print on 24 January 2011.

ME) and bred in the animal house of the Department of Biochemistry and Immunology (UFMG). Mice were $10 \pm 1$ weeks old at the time of infection. The procedures applied here have been reviewed and approved by the local animal ethics committee. Water and chow were given *ad libitum*.

*Schistosoma mansoni* strain LE used in the experiments was originally isolated from a patient in Belo Horizonte, Brazil, and has been maintained in successive passages through *Biomphalaria glabrata* snails and hamsters (*Mesocricetus auratus*) at the Laboratory of Schistosomiasis, Department of Parasitology, UFMG. Cercariae of the parasite were harvested from infected *Biomphalaria glabrata* snails, washed, counted, and injected subcutaneously into each mouse (25 cercariae per mouse) by an experienced technician (35). In the same experiment, all groups of mice were injected with the same cercaria suspension. Mortality during the infection period, which lasted 14 weeks, was observed. In any single experiment, comparisons were made only for male versus male or female versus female mice to avoid sex-dependent interferences, although no tendency toward increased mortality was observed for any sex (data not shown). Due to the high rate of mortality of CCR5-infected animals after 10 weeks of infection, the parasitological, pathological, and immunological parameters of chronically infected animals were analyzed at 11 weeks of infection. Numbers of regulatory T cells in livers and spleens of mice at 8 weeks after infection were evaluated by immunohistochemical and cytometric techniques. This time was chosen because we reasoned that regulatory events would appear before changes in pathology and mortality would occur.

**Harvesting of adult worms from the portal system.** To assess parasite burden, the circulatory system of each infected mouse was perfused after 11 weeks of *S. mansoni* infection, as described previously by Pellegrino and Siqueira (36). Worms recovered from each infected mouse were counted with the aid of a stereomicroscope. Male and female worms were morphologically identified and counted. The liver and intestine of animals subjected to perfusion were digested in 5% KOH for egg counting, as previously described (6). All other techniques discussed in following sections were applied to mice that had not been subjected to hepatic perfusion. For each technique the experiments were repeated at least twice, with similar results.

**Spleen cell culture and cytokine quantification.** For *in vitro* cell culture, infected (11 weeks of infection) and noninfected mice of both phenotypes were injected with a lethal dose of a mixture of ketamine (60 mg/kg of body weight) (Dopalen; Vetbrands) and xylazine (40 mg/kg) (Calmiun; Agener União) and bathed in a 70% alcohol solution. The abdominal wall was opened in a sterile environment, and the spleen was removed. The spleen was passed through a 70-μm cellular sieve, and the resultant cell suspension was washed and diluted in RPMI medium (Sigma) containing 5% fetal calf serum (FCS) (Cultilab), 2 mM glutamine (Sigma), 100 IU/ml K$^+$ penicillin (Pen-Syn; Wyeth), and 40 μg/ml gentamicin (Garamicina; Schering-Plough) to a concentration of $1 \times 10^7$ cells/ml after a step of erythrocyte lyses. A total of 100 μl of cell suspension was added to a 96-well plate containing soluble egg antigen (SEA) at a final concentration of 50 μg/ml or only culture medium. Soluble egg antigen was prepared from livers of *S. mansoni*-infected mice, as previously described (5). Spleen cells plated as described above were maintained for 48 h in a humidified cell incubator in the presence of air containing 5% $CO_2$. The cell supernatants were then collected for the quantification of interleukin-4 (IL-4), IL-5, IL-10, IL-13, gamma interferon (IFN-γ), CCL3, and CCL5 by an enzyme-linked immunosorbent assay (ELISA) according to the instructions supplied by the manufacturer (R&D Systems).

**Morphometric analysis of liver granulomas.** The livers from the same animals used for splenocyte cultures (11 weeks after infection) were separated, and the right lobe of each animal was readily immersed in 4% formaldehyde prepared in phosphate-buffered saline (PBS) and incubated at room temperature for 18 h, after which time the tissue samples were washed, transferred into 70% ethanol, and then paraffin embedded. Five-micrometer-thick sections were stained by the Picro-Sirius method (23). For this purpose, Direct Red 80 (Sigma) and picric acid (Synth) were used. Harris hematoxylin (Merck) was used as a counterstain. Liver sections were also stained with hematoxylin and eosin (H&E) to evaluate the inflammatory infiltration.

For the quantitative measurement of liver granulomas induced by *S. mansoni* infection in both experimental groups, images were captured with a 20× objective at a ×10 ocular magnification with a digital camera (DP12; Olympus) and analyzed with Image Pro-plus 4.0 software. Thirty or more granulomas containing a single central egg with viable miracidia were randomly selected for each animal. Fused granulomas, i.e., granulomas in which it was possible to observe more than one egg, or granulomas in which the egg was not visible or destroyed were excluded from the analysis. The granuloma area was measured with digital images using Image Pro-plus 4.0, the volume of each lesion was calculated by assuming a spherical shape, and the mean granuloma volume was plotted for each mouse (7). During the morphometric analysis of liver granulomas, we

TABLE 1. Frequency of observation of different patterns of collagen deposition on liver granulomas induced by *Schistosoma mansoni* eggs in 11-week-infected wild-type and CCR5$^{-/-}$ mice[a]

| Collagen deposition | Frequency (%) | | *P* value |
|---|---|---|---|
| | Wild-type mice | CCR5$^{-/-}$ mice | |
| Granuloma with poor collagen deposition | 4 | 6 | 0.563 |
| Granuloma with widespread collagen deposition | 61 | 54 | 0.343 |
| Granuloma with collagen deposition in the peripheral layer | 33 | 3 | **<0.001** |
| Granuloma with marked collagen deposition in the paracentral layer | 1 | 21 | **<0.001** |
| Granuloma with exuberant collagen deposition in the paracentral and peripheral layers | 1 | 16 | **<0.001** |

[a] Comparisons between groups were done by using a two-tailed Fisher exact test. Boldface type indicates statistical significance.

observed that some granulomas exhibited an unusual type of collagen distribution. To quantify this observation, the same granuloma images used to measure the reaction area were also categorized according to collagen distribution as follows: granuloma with poor collagen deposition, granuloma with widespread collagen deposition, granuloma with collagen deposition mainly in the peripheral layer, granuloma with marked collagen deposition in the paracentral layer, and granuloma with exuberant collagen deposition in the paracentral layer and peripheral layer. The percentage of each granuloma type was calculated for each mouse, and the average was plotted and analyzed for each experimental group, CCR5$^{-/-}$ and WT mice, as shown in Table 1.

Stained liver sections were also used for estimating the amount of eggs present in this tissue. To this end, the average number of eggs/field observed with a 20× objective at a ×10 ocular magnification was calculated based on 20 random fields for each mouse, giving the egg densitometric index.

The remaining liver samples obtained from each animal were kept at −70°C for the quantification of hydroxyproline and enzymatic activities.

**Quantification of *N*-acetylglucosaminidase and eosinophil peroxidase activity in liver tissue.** The enzymatic activity in liver samples of mice from both phenotypes was assayed. The activity of the *N*-acetylglucosaminidase (NAG) enzyme was used as an indirect measurement of macrophage infiltration in tissue samples, as previously shown (20), and the assay was performed after being adapted to small samples, as described elsewhere previously (3). Similarly, we used eosinophil peroxidase (EPO) activity to indirectly estimate the eosinophilic infiltration into the liver, as previously described (41, 45).

**Hydroxyproline quantification.** Liver samples of mice at 11 weeks of infection and noninfected controls were also used for hydroxyproline determination as an indirect measure of collagen content (38). To that end, tissues were homogenized in 0.9% saline, frozen at −70°C, and lyophilized. The assay was performed with 20 mg of the dry tissue, which was subjected to alkaline hydrolysis in 300 μl $H_2O$ plus 75 μl NaOH (10 M) at 120°C for 20 min. An aliquot of 50 μl of the hydrolyzed tissue was added to 450 μl of chloramine T oxidizing reagent (0.056 M chloramine T and 10% *n*-propanol in acetate-citrate buffer [pH 6.5]) and allowed to react for 20 min. A hydroxyproline standard curve was prepared in a similar manner. Color was developed by the addition of 500 μl of 1 M *p*-dimethylaminobenzaldehyde diluted in *n*-propanol–perchloric acid (2:1, vol/vol), and the absorbance was read at 550 nm. The increase in the hydroxyproline content due to *S. mansoni* infection was expressed as μg per mg of dried tissue after subtracting the hydroxyproline content of noninfected livers from mice of the same phenotype. The hydroxyproline content was also adjusted by the amount of parasite egg retained in liver. This was done by dividing the hydroxyproline concentration by the egg densitometric index obtained from the same mouse.

**Immunohistochemical and cytometric studies of spleen and liver.** In a separate experiment, mice were sacrificed just prior to the expected beginning of the mortality phase, i.e., at 8 weeks postinfection. Immunohistochemical staining of
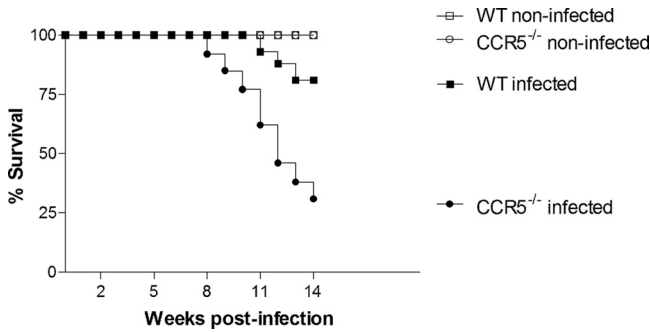
FIG. 1. Survival rates of wild-type and CCR5$^{-/-}$ mice after *S. mansoni* infection. Mice were infected with 25 cercariae, and mortality was observed for 14 weeks. There were 13 infected WT and 16 infected CCR5$^{-/-}$ mice at the beginning of the experiment. For noninfected mice (5 animals/group), the percentage of survival was 100% regardless of the phenotype or experiment ($P < 0.0001$ for comparisons of infected WT and infected CCR5$^{-/-}$ mouse survival curves). The experiment was repeated 3 times, and the mortality rate was observed during 11 to 14 weeks of infection, with similar results.

Foxp3-positive cells was done for the liver and spleen of infected mice using affinity-purified anti-mouse/anti-rat Foxp3 (clone FJK-16S; eBioscience) and a staining kit (Cell & Tissue; R&D Systems) according to the manufacturers' instructions. Positive cells were visualized by 3,3'-diaminobenzidine (DAB) staining and counted by microscopy. To confirm the immunohistochemical results obtained for the spleen, a sample of this tissue was removed and macerated through a 70-μm sieve, and cells were purified by using a Percoll gradient. Individual cell suspensions of spleens from wild-type and CCR5-deficient infected mice were stained by using fluorescein isothiocyanate (FITC) anti-CD4 (Pharmingen) and phycoerythrin (PE) anti-Foxp3 (eBioscience) and counted with a FACScan instrument (Becton Dickinson).

**Statistical analysis.** Results are expressed as means and standard errors of the means (SEM) for normally distributed data. The averages were compared by using a Student's *t* test (2 groups) or one-way analysis of variance (ANOVA), and *P* values were assigned by using Newman-Keuls *post hoc* analysis. For data presenting a nonparametric distribution, such as granuloma volume, a Mann-Whitney test was used. A Kaplan-Meier test was used to compare survival curves between *S. mansoni*-infected wild-type and *S. mansoni*-infected CCR5$^{-/-}$ mice. The frequencies of collagen deposition patterns in granulomas of infected mice from both experimental groups were compared by using a two-tailed Fisher exact test.

## RESULTS

**Infection indices for wild-type and CCR5$^{-/-}$ mice.** The lethality curves for the different groups of mice are shown in Fig.

1. In our experimental model, *S. mansoni* infection induced a low mortality rate in wild-type mice. A clear increase in the mortality rate was detected for infected CCR5$^{-/-}$ mice, reaching 70%, compared to 19% for the wild-type group at 14 weeks after infection. Death of infected CCR5$^{-/-}$ mice started at 9 weeks postinfection, i.e., around 3 to 4 weeks after the beginning of egg deposition by *S. mansoni*.

The parasite burdens of wild-type and CCR5$^{-/-}$ mice were nearly identical, with female worms being roughly half the total number of worms in either case (Fig. 2A). No statistical difference was observed for the numbers of eggs recovered from the liver (Fig. 2B) and intestine (Fig. 2C) of infected wild-type and CCR5$^{-/-}$ mice, as assessed by total tissue digestion. The number of embolized eggs in the liver and intestine of infected wild-type and CCR5$^{-/-}$ mice was also estimated by histological examination, confirming results obtained after tissue digestion (results not shown). These results suggest that the difference seen in lethality is likely a result of a role for CCR5 in pathology rather than parasite burden.

**Foxp3 expression in spleen and liver of *S. mansoni*-infected animals.** The expression of Foxp3 in the spleen and granulomatous lesions of liver from wild-type and CCR5$^{-/-}$ mice at 8 weeks postinfection was studied. Immunohistochemical analysis of spleens suggested that the number and the distribution of Foxp3-positive cells were similar in spleens from infected wild-type and CCR5$^{-/-}$ mice (Fig. 3a and b, respectively). By using flow cytometry, we confirmed that the percentages of FoxP3$^+$ CD4$^+$ lymphocytes in the spleen of *Schistosoma*-infected mice at 8 weeks were similar for wild-type and CCR5$^{-/-}$ mice (Fig. 3e). However, tissue section analysis revealed that FoxP3-positive cells were frequently found in the periphery of granulomatous lesions of wild-type *S. mansoni*-infected mice (Fig. 3d) but were rarely found in granulomas of CCR5$^{-/-}$ mice (Fig. 3c). The number of FoxP3$^+$ CD4$^+$ events in isolated granuloma cells, evaluated by flow cytometry, was very low; therefore, we evaluated FoxP3$^+$ cells recruited to the infected liver by directly counting FoxP3-positive cells in cross sections of *S. mansoni* egg-associated granulomatous lesions. As shown in Fig. 3f, a significantly lower number of FoxP3$^+$ cells was found in granulomatous lesions of tissue sections from CCR5$^{-/-}$ mice than in those from infected wild-type mice. It is also important that, at 8 weeks of infection, there was no clear difference in the granulomatous lesions observed for infected
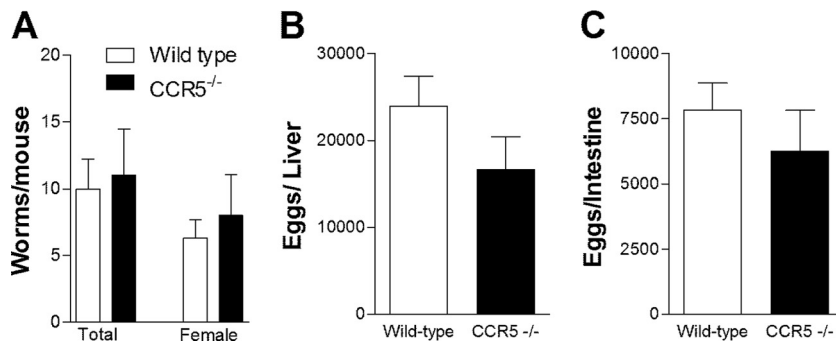


FIG. 2. Infection indices of wild-type and CCR5$^{-/-}$ mice after *S. mansoni* infection. Mice were infected with 25 cercariae and evaluated 11 weeks after infection. (A) Total number of adult or female worms recovered from the portal system. (B and C) Numbers of eggs in digested liver (B) and intestine (C). The values represent the means ± SEM from at least 8 mice per group.
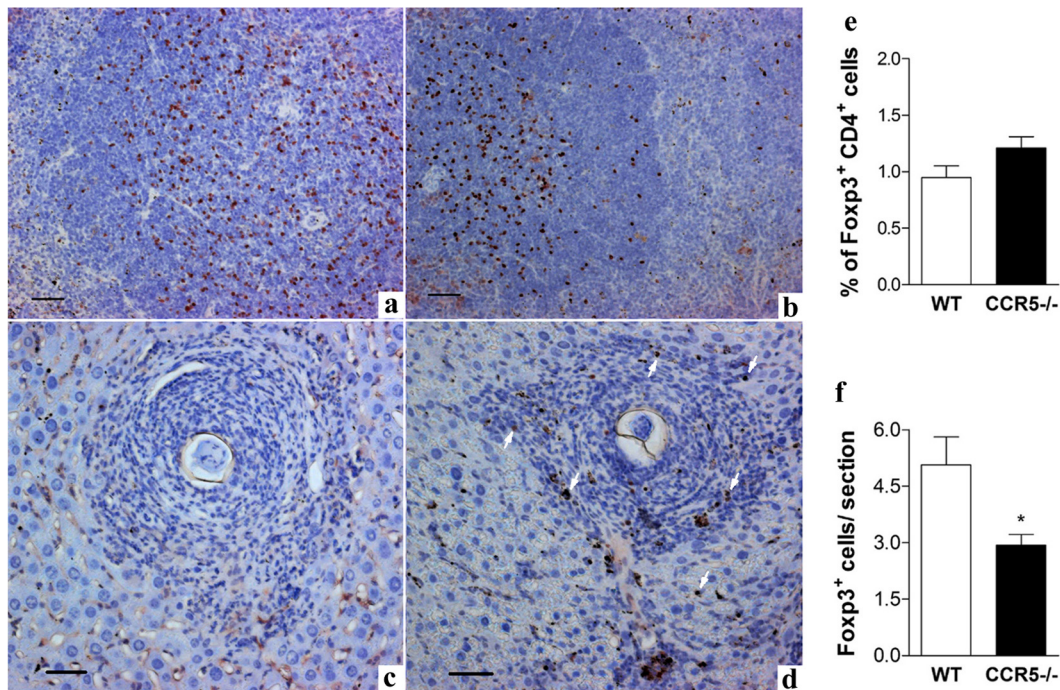
FIG. 3. FoxP3$^+$ cells in spleen and liver of wild-type and CCR5$^{-/-}$ mice after *S. mansoni* infection. Mice were infected with 25 cercariae and evaluated 8 weeks after infection. (a to d) Immunohistochemical analysis showing FoxP3$^+$ cells (brown-stained nuclei) in spleen (a and b) and in liver granulomas induced by *S. mansoni* eggs (c and d). a and c illustrated tissue from infected CCR5$^{-/-}$ mice, and b and d illustrated tissue from infected WT mice. The arrows in d indicate FoxP3$^+$ cells in the tissue section. The tissue samples were fixed with buffered formalin and embedded in paraffin, and 5-μm sections were incubated with affinity-purified anti-mouse/anti-rat Foxp3 and stained as described in Materials and Methods. Bars represent 10 μm. (e) Percentage of FoxP3$^+$ lymphocytes (FoxP3$^+$ CD4$^+$) in the spleen of infected mice from both experimental groups, estimated by cytometric analysis. (f) The number of FoxP3$^+$ cells/granuloma section was determined by the direct counting of FoxP3$^+$ cells in liver tissue. There were at least 9 animals in each group. *, $P < 0.05$ for infected wild-type versus infected CCR5$^{-/-}$ mice.

wild-type and CCR5$^{-/-}$ mice (Fig. 3c and d, respectively), and therefore, we focused our analysis of *Schistosoma*-infected mice at 11 weeks of infection.

**Hepatic inflammation in wild-type and CCR5$^{-/-}$ mice infected by *S. mansoni*.** To assess liver pathology, we first evaluated the appearance of granulomas in infected mice of both phenotypes at 11 weeks after *S. mansoni* infection. It was observed that the pattern of collagen deposition and the cellularity of the granulomatous reaction were different for each mouse phenotype, as shown in Table 1 and as illustrated in Fig. 4. The majority of granulomatous reactions found for infected mice of both phenotypes showed widespread collagen deposition (Fig. 4A2, A3, and B2). The pregranulomatous reactive stage (poor in collagen) and the granulomatous stage with widespread collagen deposition (without restricted predominance in either layer) were found with similar frequencies in mice of both phenotypes (Table 1). Wild-type mice also displayed large numbers of granulomatous reactions (over 30% of analyzed granulomas) with a more peripheral kind of collagen deposition, much in agreement with what has generally been described in the literature for liver granulomas induced by *S. mansoni* eggs (Fig. 4A4, A5, and A6). On the other hand, CCR5$^{-/-}$ mice distinguished themselves by the high number of granulomas with collagen deposition in the paracentral region (Fig. 4B5 and B6) and granulomas with exuberant collagen deposition in the paracentral and peripheral layers (Fig. 4B3 and B4). The inversion of the collagen deposition pattern

from the typical periphery-confined distribution detected in chronically WT-infected mice to the larger accumulation of collagen in the paracentral layer of granulomas observed for CCR5-deficient mice was statistically significant (Table 1).

In addition to the difference in collagen deposition, we also observed larger amounts of infiltrating cells in granulomatous reactions of infected CCR5-deficient mice (Fig. 4B4 and B5). Liver sections stained by H&E showed that granulomatous lesions of infected mice have eosinophils, fibroblasts, and other mononuclear cells. However, mononuclear cells seemed to be present in larger numbers among granulomas of infected CCR5$^{-/-}$ mice (Fig. 4B8). To support this observation, we measured enzymatic activity for eosinophil peroxidase (EPO) and macrophage *N*-acetylglucosaminidase (NAG) in livers of both experimental groups. There was a significant increase in EPO activity in livers of infected mice, which is in agreement with the large number of eosinophils observed in liver tissue by histological analysis (Fig. 4A8 and B8). However, there was no difference in EPO activity in livers of *S. mansoni*-infected CCR5$^{-/-}$ mice compared to the activity observed for infected wild-type animals (Fig. 4C). In contrast, there was a greater increase in NAG activity in the livers of infected CCR5$^{-/-}$ mice compared to wild-type mice at 11 weeks after infection (Fig. 4D), indicating that an increased number of macrophages would contribute to the greater cellularity detected in granulomatous inflammations of infected CCR5$^{-/-}$ mice.
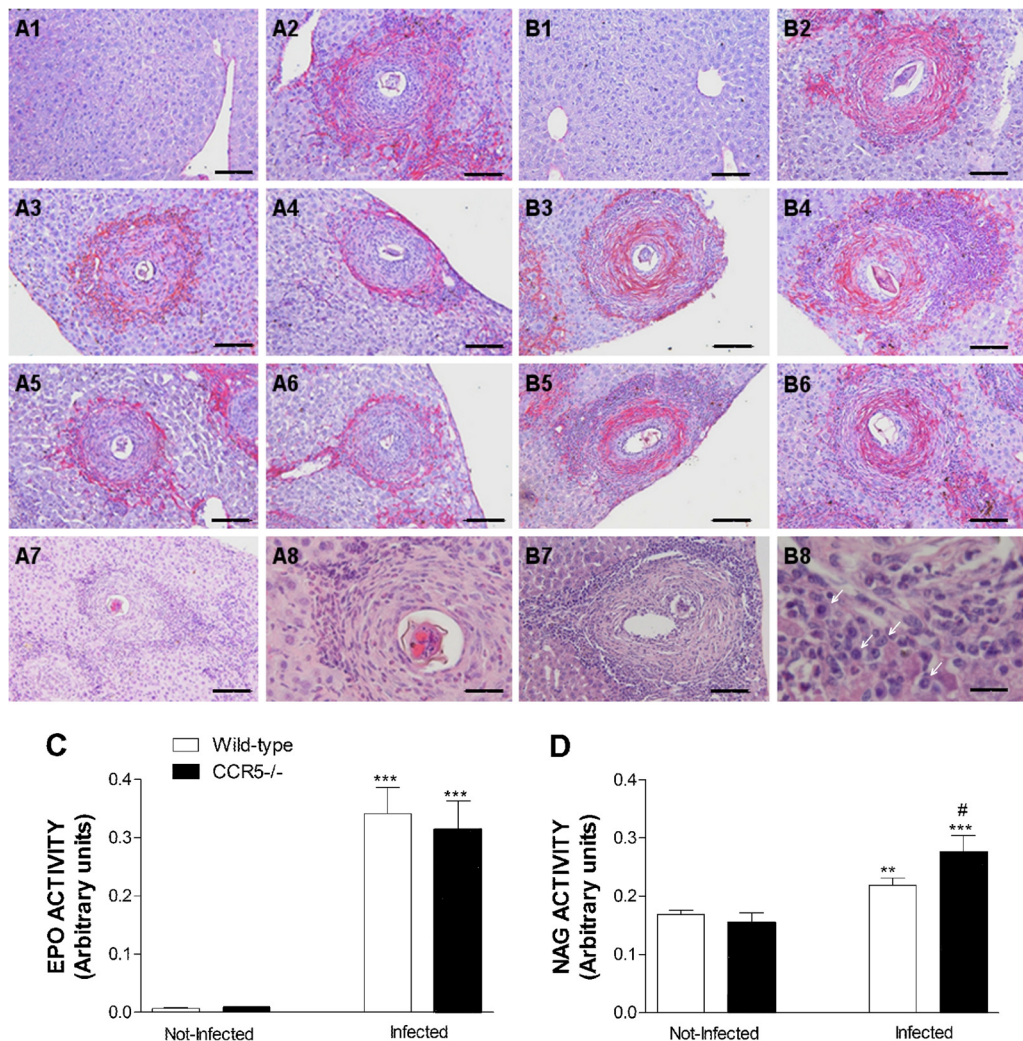
FIG. 4. Pattern of collagen deposition and cellular infiltration in liver granulomas from wild-type and CCR5$^{-/-}$ mice after *S. mansoni* infection. (A) Liver tissues and granulomatous lesions from WT mice. (A1) Appearance of the hepatic parenchyma from a noninfected wild-type mouse. (A2 and A3) Granulomatous lesion with widespread collagen deposition. (A4, A5, and A6) Granulomatous lesions with a predominance of collagen deposition in the peripheral layer. (A7 and A8) Cellular infiltration in a granulomatous lesion of an infected WT mouse. (B) Liver tissues and granulomatous lesions from CCR5$^{-/-}$ mice. (B1) Appearance of hepatic parenchyma from a noninfected CCR5$^{-/-}$ mouse. (B2) Granulomatous lesion with exuberant and widespread collagen deposition. (B3 and B4) Granulomatous lesion exhibiting exuberant collagen deposition in the paracentral and peripheral layers, separated by a zone of compact inflammatory infiltration with high cellularity. (B5 and B6) Granulomatous lesion with marked collagen deposition only in the paracentral layer. An area of extremely high cellularity is also quite visible in B5 beyond the zone of collagen deposition. (B7 and B8) Intense cellular infiltration in a granulomatous lesion of an infected CCR5$^{-/-}$ mouse, mostly mononuclear cells (arrows). Mice were infected with 25 cercariae, and liver tissues recovered from noninfected or infected mice (at 11 weeks of infection) of both phenotypes were sectioned and stained with Picro-Sirius (A1 to A6 and B1 to B6) or H&E (A7, A8, B7, and B8). Bars, 5 μm (B8), 12 μm (A8), and 50 μm (other panels).(C and D) Eosinophil peroxidase (EPO) activity (C) and *N*-acetylglucosaminidase (NAG) activity (D) in liver homogenates of noninfected and 11-week-infected wild-type and CCR5$^{-/-}$ mice. ∗∗∗, $P < 0.001$; ∗∗, $P < 0.01$ (for infected versus noninfected mice of the same phenotype). #, $P < 0.05$ for infected wild-type versus infected CCR5$^{-/-}$ mice.

To measure the differences in liver granulomatous inflammation observed for the histological analysis, we quantified the amount of hydroxyproline in the liver tissue and the volume of the granulomas in chronically infected wild-type and CCR5$^{-/-}$ mice. The data showed that the increase in the hydroxyproline concentration induced by *S. mansoni* infection was significantly higher in CCR5$^{-/-}$ mice (Fig. 5A). Moreover, the increased level of hydroxyproline content detected in livers of infected CCR5$^{-/-}$ mice was independent of the number of eggs retained in the tissue (Fig. 5B). A comparison between infected wild-type and CCR5$^{-/-}$ mice also showed that the average volume of the granulomatous reaction of CCR5$^{-/-}$ mice was statistically greater than that of wild-type mice (Fig. 5C).

***In vitro* cytokine production by splenocytes.** The concentrations of cytokines, namely, IL-4, IL-5, IL-10, IL-13, and IFN-γ (Fig. 6), were measured in the supernatant of SEA-stimulated spleen cells from normal and infected wild-type and CCR5$^{-/-}$ mice. Generally, no major cytokine production was found in the supernatant of spleen cells from noninfected mice even after SEA stimulation. Low or undetectable levels of cytokines
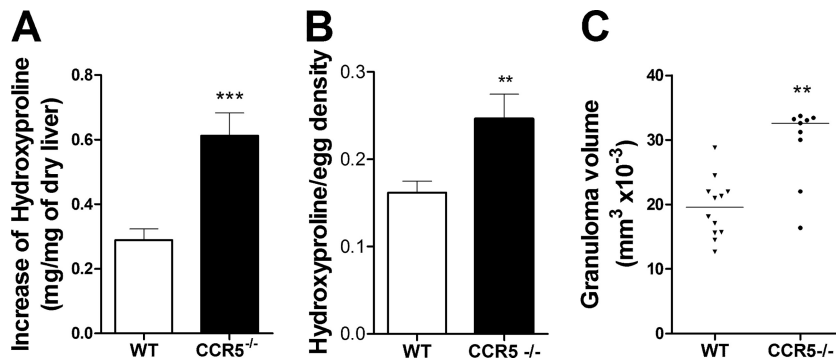
FIG. 5. *Schistosoma mansoni*-induced fibrosis and granuloma volume in livers of infected wild-type and CCR5$^{-/-}$ mice. (A and B) Fibrosis in the liver was assessed by measuring the increase of the tissue hydroxyproline content induced by infection (A) and the hydroxyproline content by egg density (B) after 11 weeks of infection in WT and CCR5$^{-/-}$ mice. (C) The granuloma volume was estimated from images of isolated granulomas containing a single viable egg at a ×200 magnification. At least 30 granulomas were captured from each animal, and there were 9 to 12 animals in each group. ∗∗∗, $P < 0.001$; ∗∗, $P < 0.01$ (for infected wild-type versus infected CCR5$^{-/-}$ mice).

were also observed for the culture supernatant from nonstimulated cells from infected mice of both groups. Stimulation with antigen induced significant increases in the levels of synthesis of IL-4 (Fig. 6A), IL-5 (Fig. 6B), IL-10 (Fig. 6C), IL-13 (Fig. 6D), and IFN-γ (Fig. 6E). When the levels of cytokines produced by stimulated cells from infected wild-type or CCR5$^{-/-}$ mice were compared against each other, statistically significant increases in levels of IL-5 and IL-13 and a decrease in the level of IL-4 was found for the CCR5$^{-/-}$ mice versus the wild-type group. The CCR5 deficiency did not affect the production of IL-10 or IFN-γ.

We have also measured the concentrations of two chemokines (CCL3 and CCL5) that are agonists of the CCR5 receptor. The stimulation of spleen cells from infected animals with SEA induced an increase in the level of secretion of CCL3 (Fig. 7A). The increase in the level of CCL3 production was greater in CCR5$^{-/-}$ mice than in wild-type mice. It is worth highlighting that CCL5 was produced by spleen cells derived from infected animals even in the absence of *in vitro* antigen stimulation (Fig. 7B). Again, the level of production of CCL5 was greater in the CCR5$^{-/-}$ group. The level of CCL3 in liver homogenates of infected animals was also greater in CCR5$^{-/-}$ mice than in wild-type mice (1,201 ± 90 pg/100 mg liver for infected WT mice and 1,755 ± 95 pg/100 mg liver for infected CCR5$^{-/-}$ mice; $P < 0.01$), while CCL5 levels in liver homogenates of infected CCR5$^{-/-}$ or wild-type mice were not different (data not shown).

## DISCUSSION

CCR5 is one of the receptors for CCL3, a chemokine previously shown to play an important role in the pathogenesis of human and murine schistosomiasis (16, 41, 42, 43). Here, we demonstrate that in the absence of CCR5, *S. mansoni* infection is severely deleterious to the host, as shown by an increase in mortality rates and egg-associated liver pathology. The lack of CCR5 resulted in larger granulomas, an enhanced deposition of collagen, and an enhanced production of IL-13, a fibrogenic cytokine. Differences in pathology and lethality were not associated with changes in parasite burden, worm fecundity, or egg

retention in the liver. The lack of CCR5 was associated with a decreased accumulation of FoxP3-positive cells.

The role of CCR5 in inflammation is controversial and apparently depends on the experimental model used. While some studies clearly demonstrated an inhibition of certain inflammatory parameters in CCR5$^{-/-}$ mice, others showed an exacerbation of inflammation in gene-deleted mice, uncovering a modulatory role of this chemokine receptor. *Toxoplasma gondii*-infected CCR5-deficient mice (26) showed less of an inflammatory response that was associated with the deficient migration of NK cells to the infection site and, consequently, lower levels of IFN-γ production. As a result, CCR5$^{-/-}$ mice were more susceptible to infection with *T. gondii* but were less susceptible to immune-mediated tissue injury. Other examples of the proinflammatory role for CCR5 include studies showing that CCR5$^{-/-}$ mice infected with *Trypanosoma cruzi* had less intense myocarditis due to the diminished migration of T cells to the heart (29) and a scarcer eosinophilic infiltrate, goblet cell hyperplasia, and diminished fibrosis after intrapulmonary challenge with *Aspergillus fumigatus* (40). Under certain experimental conditions, the CCR5 deletion can exacerbate inflammation. For instance, CCR5-deficient mice exhibited enhanced delayed-type hypersensitivity and an increase in T cell-dependent humoral responses (47), a higher level of pulmonary infiltrate after *Mycobacterium tuberculosis* infection (2), and a higher rate of liver failure-associated death after concanavalin A (Con-A) administration (1). In our experiments, the absence of CCR5 was clearly associated with enhanced granulomatous inflammation. Indeed, egg-associated granulomas in CCR5-deficient mice were larger and displayed more fibrosis and greater macrophage infiltration than those of WT mice. In addition, the patterns of collagen distribution were different for the two groups of mice. In CCR5-deficient mice, there were many granulomas in which two layers of collagen deposition were observed, suggesting a more aggressive behavior of the granulomatous response. This enhanced granulomatous response was associated with an enhanced lethality rate, suggesting that it was contributing to the death of animals. Similar findings were observed previously for *S. mansoni*-infected IL-13Rα2-deficient mice, in which there was enhanced liver pa-
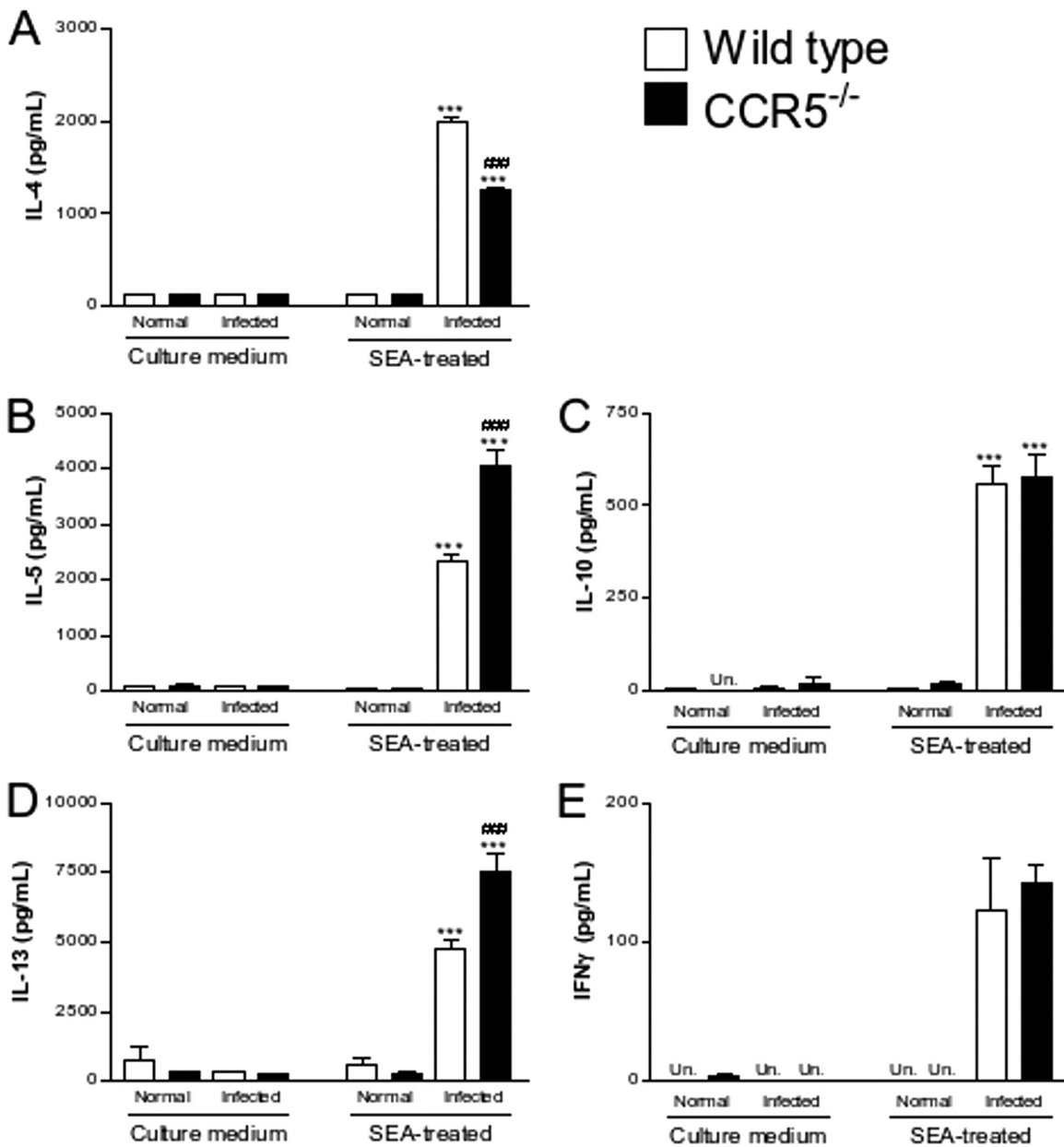
FIG. 6. Cytokine production by splenocytes from wild-type and CCR5$^{-/-}$ mice after *S. mansoni* infection. Mice were infected with 25 cercariae and evaluated 11 weeks after infection. IL-4 (A), IL-5 (B), IL-10 (C), IL-13 (D), and IFN-$\gamma$ (E) concentrations were determined by ELISA for the supernatants of spleen cells cultured in the absence (culture medium) or presence (SEA treated) of *Schistosoma* egg antigen. The values represent the averages ± SEM for 4 mice in each group. ***, $P < 0.001$ for infected versus noninfected mice of the same phenotype; ###, $P < 0.001$ for infected wild-type versus infected CCR5$^{-/-}$ mice. Un, not detectable.

thology that was associated with enhanced lethality rates (32). As the enhanced granulomatous response appeared to contribute to disease severity, we investigated molecular and cellular markers associated with this enhanced response.

The stimulation of splenocytes from infected mice with egg antigens showed an enhanced production of IL-13. The role of IL-13 in *S. mansoni*-induced fibrosis is well established for mice (8, 9, 10, 17, 25, 31, 32), results which have been confirmed for humans (12, 14, 30). In contrast, IL-4 does not seem to be essential for the liver fibrosis induced by egg deposition (22). Indeed, studies with IL-13R$\alpha$1-deficient mice show de-

creased granulomatous inflammation with poor collagen deposition and reduced rates of mortality (37). Therefore, the enhanced secretion of IL-13 observed for CCR5$^{-/-}$ mice may have contributed to the exacerbated granulomatous response and increased lethality.

Regulatory T cells express multiple chemokine receptors (28). Nonetheless, data from studies with humans and experimental animals have suggested that CCR5 may be particularly important for regulatory cells exhibiting a high level of effector function (24, 33). Moreover, for mice infected with *Leishmania major*, it was shown previously that CCR5 expression favors
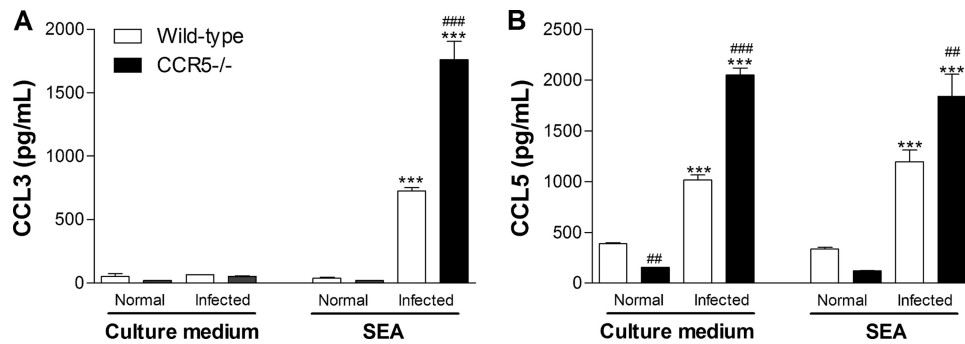
FIG. 7. Chemokine production from wild-type and CCR5$^{-/-}$ mice after *S. mansoni* infection. Mice were infected with 25 cercariae and evaluated 11 weeks after infection. CCL3 (A) and CCL5 (B) concentrations in the supernatants of spleen cells cultured in the absence (culture medium) or presence (SEA treated) of *Schistosoma* egg antigen were determined by ELISA. The values represent the averages ± SEM for 4 mice in each group. ∗∗∗, $P < 0.001$ for infected versus noninfected mice of the same phenotype. ##, $P < 0.01$; ###, $P < 0.001$ (for wild-type versus CCR5$^{-/-}$ mice at the same time point in infection).

the recruitment of cells with regulatory properties to the infection site, leading to the persistence of the parasites in the skin (46). Recently (27), it was demonstrated with *H. capsulatum*-infected mice that CCR5 influenced Treg homing and proliferation in the lung. Considering the suggested role of CCR5 in the recruitment of regulatory T cells to sites of inflammation, we examined the expression of FoxP3 in cells from spleens and livers of infected wild-type and CCR5$^{-/-}$ mice. The evaluation was done 8 weeks after experimental infection, because we reasoned that regulatory events would appear before changes in pathology and mortality would occur. Even though we detected similar proportions of FoxP3$^+$ cells in spleens of infected mice, there was a reduction in the recruitment of FoxP3$^+$ cells into the liver granulomas of infected CCR5$^{-/-}$ mice. We have not investigated in detail the phenotype of FoxP3$^+$ cells. However, these results suggest that the recruitment of FoxP3$^+$ cells, many of which are T regulatory cells and have regulatory function, is decreased in the liver of CCR5-deficient mice. Therefore, the decreased recruitment of cells with a regulatory phenotype into the granulomatous lesion of *S. mansoni*-infected CCR5$^{-/-}$ mice may also account for the increased pathology and lethality detected in our experimental model.

Another interesting finding with mechanistic implications was the demonstration that there were elevated levels of CCR5 ligands, especially CCL3, in infected CCR5-deficient mice. Levels of CCL3 are associated with more severe disease in humans infected with *S. mansoni*, and infected CCL3-deficient mice have less disease (42). In addition to CCR5, CCL3 may bind to other receptors, especially CCR1 (34). It was demonstrated previously that lung granulomas induced by the intravenous injection of *S. mansoni* eggs were smaller in CCR1-deficient mice than in wild-type controls (19), suggesting that CCR1 plays a positive role in controlling granuloma size. Therefore, the observed increase in levels of CCL3 may contribute to disease severity by stimulating CCR1, even in the absence of CCR5. However, why were levels of CCL3 increased? A previous study by Cardona and colleagues (4) provided an interesting mechanistic insight. Those authors showed that chemokine receptors may function as scavengers of the chemokines to which they bind. In the absence of CCR5, chemokines which bind to CCR5, including CCL3 and CCL5,

may be enhanced in the circulation and tissues and bind to their other receptors, including CCR1. In our experimental situation, higher levels of CCL3 in *S. mansoni*-infected CCR5-deficient mice could now activate CCR1 and contribute to the observed enhancement of granulomatous inflammation.

In conclusion, we have shown here that the CCR5 deletion is deleterious to the mouse host in the course of *S. mansoni* infection. This fact is evidenced by the increased lethality rates and in worsened disease parameters, including the increased production of IL-13, enhanced granuloma size, and alterations in the amount and pattern of collagen deposition around the eggs. Mechanistically, the absence of CCR5 caused a reduction of the recruitment of FoxP3$^+$ cells to granulomatous lesions, increased levels of CCL3, and enhanced macrophage infiltration in liver, suggesting a modulatory role for CCR5 in the context of *S. mansoni* infection.

## REFERENCES

1. **Ajuebor, M. N., et al.** 2005. Lack of chemokine receptor CCR5 promotes murine fulminant liver failure by preventing the apoptosis of activated CD1d-restricted NKT cells. J. Immunol. **174:**8027–8037.
2. **Algood, H. M., and J. L. Flynn.** 2004. CCR5-deficient mice control *Mycobacterium tuberculosis* infection despite increased pulmonary lymphocytic infiltration. J. Immunol. **173:**3287–3296.
3. **Barcelos, L. S., et al.** 2005. Impaired inflammatory angiogenesis, but not leukocyte influx, in mice lacking TNFR1. J. Leukoc. Biol. **78:**352–358.
4. **Cardona, A. E., et al.** 2008. Scavenging roles of chemokine receptors: chemokine receptor deficiency is associated with increased levels of ligand in circulation and tissues. Blood **112:**256–263.
5. **Carter, C. E., and D. G. Colley.** 1978. An electrophoretic analysis of *Schistosoma mansoni* soluble egg antigen preparation. J. Parasitol. **64:**285–290.
6. **Cheever, A. W.** 1968. Conditions affecting accuracy of potassium hydroxide digestion techniques for counting *Schistosoma mansoni* eggs in tissues. Bull. World Health Organ. **39:**328–331.

7. **Cheever, A. W., et al.** 1987. Variation of hepatic fibrosis and granuloma size among mouse strains infected with Schistosoma mansoni. Am. J. Trop. Med. Hyg. **37:**85–97.

8. **Chiaramonte, M. G., A. W. Cheever, J. D. Malley, D. D. Donaldson, and T. A. Wynn.** 2001. Studies of murine schistosomiasis reveal interleukin-13 blockade as a treatment for established and progressive liver fibrosis. Hepatology **34:**273–282.

9. **Chiaramonte, M. G., D. D. Donaldson, A. W. Cheever, and T. A. Wynn.** 1999. An IL-13 inhibitor blocks the development of hepatic fibrosis during a T-helper type 2-dominated inflammatory response. J. Clin. Invest. **104:**777–785.

10. **Chiaramonte, M. G., et al.** 1999. IL-13 is a key regulatory cytokine for Th2 cell-mediated pulmonary granuloma formation and IgE responses induced by *Schistosoma mansoni* eggs. J. Immunol. **162:**920–930.

11. **Dairaghi, D. J., et al.** 1998. Macrophage inflammatory protein-1beta induces migration and activation of human thymocytes. Blood **91:**2905–2913.

12. **de Jesus, A. R., et al.** 2004. Association of type 2 cytokines with hepatic fibrosis in human *Schistosoma mansoni* infection. Infect. Immun. **72:**3391–3397.

13. **Deng, H., et al.** 1996. Identification of a major co-receptor for primary isolates of HIV-1. Nature **381:**661–666.

14. **Dessein, A., et al.** 2004. Interleukin-13 in the skin and interferon-gamma in the liver are key players in immune protection in human schistosomiasis. Immunol. Rev. **201:**180–190.

15. **Dragic, T., et al.** 1996. HIV-1 entry into CD4+ cells is mediated by the chemokine receptor CC-CKR-5. Nature **381:**667–673.

16. **Falcão, P. L., et al.** 2002. Plasma concentrations and role of macrophage inflammatory protein-1alpha during chronic *Schistosoma mansoni* infection in humans. J. Infect. Dis. **186:**1696–1700.

17. **Fallon, P. G., E. J. Richardson, G. J. McKenzie, and A. N. McKenzie.** 2000. Schistosome infection of transgenic mice defines distinct and contrasting pathogenic roles for IL-4 and IL-13: IL-13 is a profibrotic agent. J. Immunol. **164:**2585–2591.

18. **Fritsch, L., et al.** 1998. Production of HIV-1 by human B cells infected in vitro: characterization of an EBV genome-negative B cell line chronically synthesizing a low level of HIV-1 after infection. Virology **244:**542–551.

19. **Gao, J. L., et al.** 1997. Impaired host defense, hematopoiesis, granulomatous inflammation and type 1-type 2 cytokine balance in mice lacking CC chemokine receptor 1. J. Exp. Med. **185:**1959–1968.

20. **Green, A. P., F. Mangan, and J. E. Ormerod.** 1980. Induction of cell infiltration and acid hydrolase release into the peritoneal cavity of mice. Inflammation **4:**205–213.

21. **Huang, Y., et al.** 1996. The role of a mutant CCR5 allele in HIV-1 transmission and disease progression. Nat. Med. **2:**1240–1243.

22. **Jankovic, D., et al.** 1999. Schistosome-infected IL-4 receptor knockout (KO) mice, in contrast to IL-4 KO mice, fail to develop granulomatous pathology while maintaining the same lymphokine expression profile. J. Immunol. **163:**337–342.

23. **Junqueira, L. C., G. Bignolas, and R. R. Brentani.** 1979. Picrosirius staining plus polarization microscopy, a specific method for collagen detection in tissue sections. Histochem. J. **11:**447–455.

24. **Kang, S. G., et al.** 2007. Identification of a chemokine network that recruits FoxP3(+) regulatory T cells into chronically inflamed intestine. Gastroenterology **132:**966–981.

25. **Kaviratne, M., et al.** 2004. IL-13 activates a mechanism of tissue fibrosis that is completely TGF-beta independent. J. Immunol. **173:**4020–4029.

26. **Khan, I. A., et al.** 2006. CCR5 is essential for NK cell trafficking and host survival following Toxoplasma gondii infection. PLoS Pathog. **2:**e49.

27. **Kroetz, D. N., and G. S. Deepe, Jr.** 2010. CCR5 dictates the equilibrium of proinflammatory IL-17+ and regulatory Foxp3+ T cells in fungal infection. J. Immunol. **184:**5224–5231.

28. **Lim, H. W., J. Lee, P. Hillsamer, and C. H. Kim.** 2008. Human Th17 cells share major trafficking receptors with both polarized effector T cells and FOXP3+ regulatory T cells. J. Immunol. **180:**122–129.

29. **Machado, F. S., et al.** 2005. CCR5 plays a critical role in the development of myocarditis and host protection in mice infected with *Trypanosoma cruzi*. J. Infect. Dis. **191:**627–636.

30. **Magalhães, A., et al.** 2004. Cytokine profile associated with human chronic schistosomiasis mansoni. Mem. Inst. Oswaldo Cruz **99:**21–26.

31. **McKenzie, G. J., P. G. Fallon, C. L. Emson, R. K. Grencis, and A. N. McKenzie.** 1999. Simultaneous disruption of interleukin (IL)-4 and IL-13 defines individual roles in T helper cell type 2-mediated responses. J. Exp. Med. **189:**1565–1572.

32. **Mentink-Kane, M. M., et al.** 2004. IL-13 receptor alpha 2 down-modulates granulomatous inflammation and prolongs host survival in schistosomiasis. Proc. Natl. Acad. Sci. U. S. A. **101:**586–590.

33. **Moreira, A. P., et al.** 2008. CCR5-dependent regulatory T cell migration mediates fungal survival and severe immunosuppression. J. Immunol. **180:**3049–3056.

34. **Murphy, P. M., et al.** 2000. International Union of Pharmacology. XXII. Nomenclature for chemokine receptors. Pharmacol. Rev. **52:**145–176.

35. **Pellegrino, J., and D. G. Macedo.** 1955. A simplified method for concentration of cercarial. J. Parasitol. **41:**306–309.

36. **Pellegrino, J., and A. F. Siqueira.** 1956. A perfusion technic for recovery of *Schistosoma mansoni* from experimentally infected guinea pigs. Rev. Bras. Malariol. Doencas Trop. **8:**589–597.

37. **Ramalingam, T. R., et al.** 2008. Unique functions of the type II interleukin 4 receptor identified in mice lacking the interleukin 13 receptor alpha1 chain. Nat. Immunol. **9:**25–33.

38. **Reddy, G. K., and C. S. Enwemeka.** 1996. A simplified method for the analysis of hydroxyproline in biological tissues. Clin. Biochem. **29:**225–229.

39. **Samson, M., O. Labbe, C. Mollereau, G. Vassart, and M. Parmentier.** 1996. Molecular cloning and functional expression of a new human CC-chemokine receptor gene. Biochemistry **35:**3362–3367.

40. **Schuh, J. M., K. Blease, and C. M. Hogaboam.** 2002. The role of CC chemokine receptor 5 (CCR5) and RANTES/CCL5 during chronic fungal asthma in mice. FASEB J. **16:**228–230.

41. **Souza, P. R., A. L. Souza, D. Negrão-Correa, A. L. Teixeira, and M. M. Teixeira.** 2008. The role of chemokines in controlling granulomatous inflammation in *Schistosoma mansoni* infection. Acta Trop. **108:**135–138.

42. **Souza, A. L., et al.** 2005. Potential role of the chemokine macrophage inflammatory protein 1-alpha in human and experimental schistosomiasis. Infect. Immun. **73:**2515–2523.

43. **Souza, A. L., S. R. Sousa-Pereira, M. M. Teixeira, J. R. Lambertucci, and A. L. Teixeira.** 2006. The role of chemokines in *Schistosoma mansoni* infection: insights from human disease and murine models. Mem. Inst. Oswaldo Cruz **101:**333–338.

44. **Sozzani, S., et al.** 1997. Receptor expression and responsiveness of human dendritic cells to a defined set of CC and CXC chemokines. J. Immunol. **159:**1993–2000.

45. **Strath, M., D. J. Warren, and C. J. Sanderson.** 1985. Detection of eosinophils using an eosinophil peroxidase assay. Its use as an assay for eosinophil differentiation factors. J. Immunol. Methods **83:**209–215.

46. **Yurchenko, E., et al.** 2006. CCR5-dependent homing of naturally occurring CD4+ regulatory T cells to sites of Leishmania major infection favors pathogen persistence. J. Exp. Med. **203:**2451–2460.

47. **Zhou, Y., et al.** 1998. Impaired macrophage function and enhanced T cell-dependent immune response in mice lacking CCR5, the mouse homologue of the major HIV-1 coreceptor. J. Immunol. **160:**4018–4025.